IMPACTS OF SUBSTITUTING Ni^{2+} IONS ON STRUCTURAL AND ELECTRICAL PROPERTIES OF W-TYPE BARIUM BASED HEXAFERRITES

N. AMIN[a], R. BILAL[a], G. MUSTAFA[b], A. ASLAM[a], M. S. HASAN[c],
K. HUSSAIN[a], M. TABASSUM[a], M. FATIMA[a], Z. E. KHAN[a], A. NASEEM[a],
M. AKHTAR[a], M. GULZAR[a], I. YOUNAS[a], S. AMIN[a], S. SHAKEEL[a],
QURAT-UL-AIN[a], M. I. ARSHAD[a,*]

[a]*Department of Physics, Government College University, Faisalabad 38000, Pakistan*
[b]*Department of Physics, Bahauddin, Zakariya University Multan, 60800, Pakistan*
[c]*Department of Physics, The University of Lahore, 1-kM Raiwind Road, Lahore, Pakistan*

W-type Barium based ferrites with composition $BaZn_{2-x}Ni_xFe_{16}O_{27}$ for (x = 0.0, 0.1, 0.2, 0.3, 0.4) were synthesized by chemical co-precipitation technique by 8h sintering at 1100^{0}C in order to investigate their structural and electrical properties. XRD patterns confirmed the formation of w type phase. It was observed that, initially the crystallite size increased from 15.285nm to 16.056nm with increasing concentration of nickel up to x = 0.1 but then gradually decreased to 15.68nm up to x = 0.4. This decrease showed that nickel act as crystallite inhibitor. Lattice constants decrease with increasing concentrations of substituted ions attributed to the fact that ionic radius of nickel (0.069nm) is less than that of zinc (0.072nm). X-ray density increased from 2.43 to 2.50g/cm^3 with increase in nickel concentration up to x = 0.3 and then decrease to 2.47g/cm^3. As the atomic weight of nickel (58.69 amu) is smaller than zinc (65.37 amu). So the X-ray density should decrease with increasing nickel contents but here increase contradicted which may be due to variations in lattice distortions. FTIR spectra showed three frequency bands corresponding to tetrahedral, N-O stretching vibration of NO_3 ions, stretching and twisting of $^-$OH surface hydroxy group respectively. Resistivity increased with increase in nickel concentration from 0.59×10^7 Ω cm to 5.45×10^7 Ω cm.

1. Introduction

In 1957 Braun discovered the crystal structure of W-type ferrites having chemical formula $BaMe_2Fe_{16}O_{27}$, in which Me is any divalent metal ion. The presence of these metal ions in w type structure permits greater chances of varying the electrical characteristics with appropriate variety of cations in comparison of M-type crystal structure [1,2]. A change in Me^{2+} cations makes them feasible to be used as a permanent magnet having high energy product than BaM [3]. The unit cell of these ferrites belongs to P6$_3$/mmc [4] and formed by superposition of two spinel and one R (a block containing Ba ions) blocks together with the hexagonal c-axis i.e RSSR*S*S*, the asterik indicates that the corresponding blocks are turned out through 180^0 along the hexagonal axis [5-8]. Presence of an easy axis (c-axis) makes them anisotropic as it is simpler to adjust the spin directions about c-axis that is normal to the hexagonal basel plane [9].

Electrical characteristics of hard ferrites have very importance as these ferrites have applications at GHz frequencies [10]. Up to now few researches are available about the electrical characteristics of W-type ferrites [11-16]. Aen *et al.* [17] reported increase in electrical resistivity (3.01× 10^9 to 5.69× 10^{10} Ωcm) of Ho^{3+} substituted barium based ferrites (BaCo$_2$Fe$_{16}$O$_{27}$) with increase in Ho^{3+} contents. Ahmad et al. [18] have studied electrical properties of La substituted

---

hexaferrites ($BaZn_2La_xFe_{16-x}O_{27}$) and found an increase in electrical resistivity from 0.59×10^7 to $8.42 \times 10^7 \Omega$ cm. Iqbal et al. [19] found an increase in electrical resistivity of Cr substituted ferrites ($BaZn_2Cr_xFe_{16-x}O_{27}$) from 3.25×10^8 to $2.79 \times 10^9 \Omega$ cm. No study was found about the electrical properties of Ni substituted W-type barium based ferrites.

In this research paper effect of Ni substitution on structural parameters (lattice constants, X-ray density, crystallite size) and electrical resistivity of W-type barium based ferrites prepared by co-precipitation technique by 8h sintering at 1100^oC was studied.

2. Experimental procedure

For the synthesis of W-type barium based hexaferrites with chemical formula $BaZn_{2-x}Fe_{16}O_{27}$ (x = 0.0-0.4) by co-precipitation method, $BaCl_2.2H_2O$ (244.26g/mol), $ZnCl_2$ (136.30g/mol), $NiCl_2.6H_2O$ (237.69g/mol), $Fe(NO_3)_3.9H_2O$ (403.99g/mol) were used as raw materials. Digital electronic balance was used for measuring the stochiometric amounts of all chemicals. Each chemical was dissolved in 100 ml distilled water in a separate beaker .Then all solutions were combined in one beaker and placed on a magnetic stirrer at moderate constant stirring speed (60 rpm) and 100^0C temperature. After 1h of vigorous stirring, the solution of 12g NaOH in 100ml distilled water was added drop wise into the salts solution until the desired pH 10 was obtained. After 1h constant stirring, co-precipited solutions were allowed to cool down at room temperature and then placed in water bath for 2h at 90^0C so that co-precipitates settled down. Through the process of filteration, obtained particles were washed 3 to 4 times with distilled water and accetone until neutral pH 7 was obtained and dried in an electric oven at 90^0C over night. The fine dried material was obtained by 3h grinding of dried material using pestle and mortar. The resulted samples were poured into the crucibles and calcined in a tube furnace at a rate of 5^0C/min for 8h at 1100^oC. Powder samples were pressed into the pellets by using dye and hydraulic press to characterize the electrical characteristics of the prepared samples.

3. Results and discussion

3.1. XRD analysis

XRD pattern for samples prepared at 1100^0C by 8h sintering through co-precipitation method is shown in Fig. 1. Matching of these patterns with JCPDS card no COD 1008955 confirmed the formation of W-type barium based ferrites with hexagonal crystal structure belonging to space group P 6_3/mmc. Ni^{2+} phases were not observed in these patterns, showing the entrance of Ni^{2+} into crystalline lattice [20].
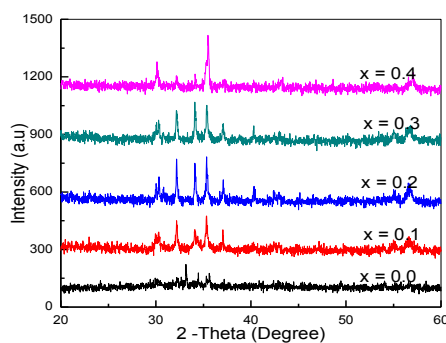

Fig. 1. XRD Patterns for $BaZn_{2-x}Ni_xFe_{16}O_{27}$ for (x = 0.0, 0.1, 0.2, 0.3, 0.4) ferrites.

Lattice parameters (a) and (c) are determined by using the values of interplaner spacing (d_{hkl}) according to equation:

$$d_{hkl} = \left(\frac{4}{3} \left(\frac{h^2 + hk + k^2}{a^2} \right) + \frac{l^2}{2} \right)^{-\frac{1}{2}} \tag{1}$$

which illustrates relation between interplanar spacing and lattice parameters (a, c) in which d_{hkl} represents inter planer spacing and h, k and l are miller indices [21, 22]. Fig. 2 and 3 depicts relation between lattice parameters (a, c) and Ni^{2+} concentration, respectively. Both lattice constants decrease with increase in nickel concentration, attributed to the fact that ionic radius of Ni^{2+} (0.069nm) is small as compared to Zn^{2+} (0.072nm). Crystallite size is calculated by scherrer formula:

$$D = \frac{k\lambda}{\beta_{hkl} cos\theta} \tag{2}$$

where, $\lambda = 1.5406$ Å is the wavelength of X-ray diffraction, θ is the Bragg's diffraction angle, k is the shape factor, its value is 0.9, while β_{hkl} is full width at half maximum (FWHM). Fig 4. shows variations in crystallite size with increase in nickel contents.

Initially the crystallite size of barium based ferrites ($BaZn_{2-x}Ni_xFe_{16}O_{27}$) for x = 0.0 was 15.285nm and with nickel substitution (x=0.1) crystallite size increased to 16.056nm. Then gradually decreased to 15.68nm as nickel concentration increased up to x= 0.4. This decrease in crystallite size with nickel concentration shows that nickel act as crystallite inhibitor. X-ray density determined from the formula:

$$D_x = \frac{2M}{N_A V} \tag{3}$$

where, 2 represents number of molecules per unit cell, M is the molecular weight of the sample, N_A is the Avogadro's number (6.02×10^{23} g/mol) and V is the unit cell volume [1]. Where, V_{cell} and d-values are calculated by the relations:

$$V_{cell} = a^2 c Sin(120°) \tag{4}$$

$$2dsin\theta = n\lambda \tag{5}$$

Fig. 4 shows relationship between concentration of nickel and X-ray density of barium based ferrites. With increase in nickel concentration X-ray density increased up to 2.50g/cm^3 for x = 0.3. As atomic weight of nickel (58.69amu) is less than that of Zinc (65.37amu) so X-ray density should decrease with increase in the substituted ions but results are in contradiction with literature. This contradiction may be due to variations in lattice distortions with increase in the concentration of nickel. When the nickel concentration increase d further (x = 0.4) X-ray density decreased to 2.47g/cm^3.

Table 1. Lattice constant (a and c), Crystallite size (D), X-ray density (D_x) of $BaZn_{2-x}Ni_xFe_{16}O_{27}$ for (x = 0.0, 0.1, 0.2, 0.3, 0.4) ferrites.

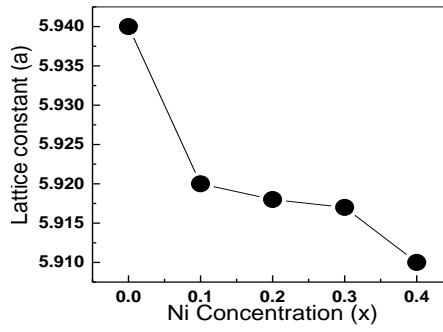| Sr. No	Ni^{2+} Content (x)	a (Å)	c (Å)	D (nm)	D_x (g/cm^3)
1	0.0	5.940	33.145	15.285	2.43
2	0.1	5.920	33.034	16.056	2.44
3	0.2	5.918	33.021	16.009	2.47
4	0.3	5.917	33.018	15.960	2.50
5	0.4	5.910	32.994	15.680	2.47

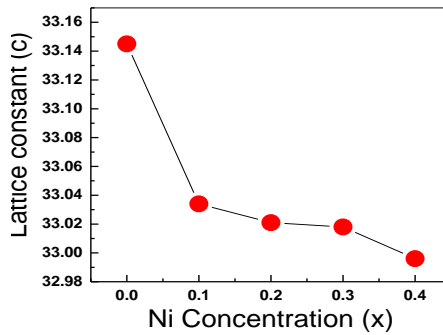*Fig. 2. Graph between nickel concentration and lattice constant (a).*

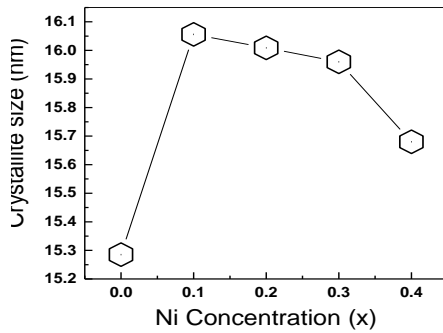*Fig. 3. Graph between nickel concentration and lattice constant (c).*

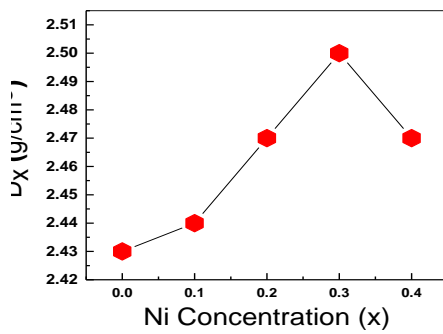*Fig. 4. Graph between Nickel concentration and average crystallite size.*

Fig. 5. Graph between Nickel concentration and X_{ray}–Density.

3.2. Fourier transform infrared spectra for Ni-Zn W hexaferrites

Fourier transform infrared absorption spectra of $BaZn_{2-x}Ni_xFe_{16}O_{27}$ for Ni contents 0.0, 0.1, 0.2, 0.3, 0.4 are shown in Fig. 6. The spectra were recorded in the range of 500 – 4000 nm. These spectra revealed three characteristics absorption bands. Out of which, first band is due to tetrahedral group owing to vibrations of Fe^{3+}-O^{2-} bond. The second band is attributed to the N-O stretching vibration of NO_3 ions. The third band shows the stretching and twisting bands of -OH surface hydroxy group of nanoparticles attained from wet environment during the process of synthesis.
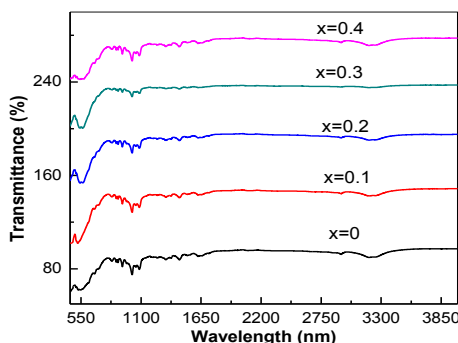

Fig. 6. FTIR spectra of $BaZn_{2-x}Ni_xFe_{16}O_{27}$ for (x = 0.0, 0.1, 0.2, 0.3, 0.4)ferrites.

Table 2. FTIR band spectrum for tetrahedral group (V_1), N-O stretching vibration (V_2) and -OH surface hydroxy group (V_3) of nanoferrites.

Sr. No.	Concentration Wt. (%)	Frequency band (v_1) nm	Frequency band (v_2) nm	Frequency band (v_3) nm
1	X = 0.0	552.35	1020.16	2937.30
2	X = 0.1	555.09	1020.66	2932.70
3	X = 0.2	552.35	1011.96	2928.78
4	X = 0.3	542.51	1015.76	2935.58
5	X = 0.4	525.67	1017.46	2931.76

3.3. I-V analysis for Ni- Zn W hexaferrites

Electrical resistivity of barium based ferrites ($BaZn_{2-x}Ni_xFe_{16}O_{27}$) with nickel content 0.0, 0.1, 0.2, 0.3, 0.4 is calculated from I-V curves by using the formula:

$$R = \frac{\rho L}{A} \tag{5}$$

In which R is the resistance, A is the area and L is the width of the pellet. Fig. 7 shows variations in resistivity of barium based ferrites with nickel concentration.
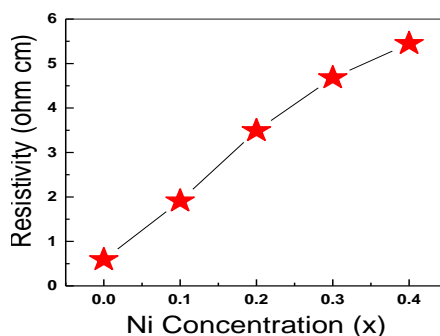

Fig. 7. Resistivity vs. Ni concentration of nanoferrites.

From this graph it is clear that with increase in nickel concentration from x = 0.0 to x = 0.5 resistivity of barium based ferrites increased from 0.59×10^7 to 5.451×0^7. Increase in resistivity make these ferrites promising for use at higher frequencies.

Table 3. Resistivity of $BaZn_{2-x}Ni_xFe_{16}O_{27}$ for (x = 0.0, 0.1, 0.2, 0.3, 0.4) nanoferrites.

Sr. No	Nickel concentration (x)	Resistivity (Ω cm)
1	0.0	0.591×0^7
2	0.1	1.911×0^7
3	0.2	3.49×10^7
4	0.3	4.68×10^7
5	0.4	5.45×10^7

4. Conclusion

Barium based ferrites with composition $BaZn_{2-x}Ni_xFe_{16}O_{27}$ for (x = 0.0-0.4) were prepared by co-precipitation method. XRD patterns confirmed the formation of W type ferrites with some impurity phases such as αFe_2O_3 due to low sintering temperature. Ni^{2+} phases were not appeared, showing its entrance into crystalline lattice. Lattice constants (a, c) decreased with increase in nickel concentration. Crystallite size increased to 16.056nm for x= 0.1 but then decreased to 15.68nm upto x= 0.4. X-ray density increased with increase in nickel concentration in contradiction with literature, which may be due to variations in lattice distortions with increase in nickel concentration. FTIR spectra showed three absorption bands. I-V analysis showed increase in resistivity from $0.59 \times 10^7 \Omega$ cm to $5.45 \times 10^7 \Omega$ cm. Increase in resistivity making these ferrites promising for use at high frequencies.

References

[1] D. M. Hemeda et al., Journal of Magnetism and Magnetic Materials **315**(1), 1 (2007).
[2] Y. Wu et al., Journal of Magnetism and Magnetic Materials. **324**(4), 616 (2012).
[3] S. P. Sawadh, K. D. Kulkarni., Journal of Materials Chemistry and Physics **63** (2), 170 (2000).
[4] C. Ri et al., Journal of Magnetism and Magnetic Materials **324**, 1498 (2012).
[5] H. P. Wijn et al., Le Journal de Physique Colloques. **38**, C1-85 (1977).
[6] D. El. Kony, S. A. Saafan., Journal of Magnetism and Magnetic Materials **267**(1), 46 (2003).
[7] R. B. Jotania et al., Journal of Magnetism and Magnetic Material **320**, 1095 (2008).
[8] R. C. Pullar, J. Prog., Journal of Materials Science **57,** 1191 (2017).
[9] M. Ahmad et al., Journal of Magnetism and Magnetic Materials **332,** 137 (2013).
[10] M. A. Ahmed et al., Journal of Magnetism and Magnetic Materials **321** (24), 3967 (2009).
[11] Y. Nie et al., Journal of Magnetism and Magnetic Materials **303,** 423 (2006).
[12] S. M. Attia et al., Journal of Magnetism and Magnetic Materials **270**, 142 (2004).
[13] A. M. Abo El Ata, M. A. Ahmad., Journal of Magnetism and Magnetic Materials **208** (1), 27 (2000).
[14] X. H. Wang et al., Journal of Magnetism and Magnetic Materials **184,** 95 (1998).
[15] R. C. Pullar et al., Journal of Materials Science **17**, 973 (1998).

[16] K. L. Wauchi, Y. Ikeda., Journal of Physica Status Solidi A **93**, 309 (1986).
[17] F. Aen et al., Journal of Ceramics International **42** (14), 16077 (2016).
[18] M. Ahmad et al., Journal of Ceramics International **37**(8), 3691 (2011).
[19] M. J. Iqbal, R. A. Khan., Journal of Alloys Compound. **478**(1-2), 847 (2009).
[20] L. Deng et al., Journal of Magnetism and Magnetic Materials **323**(14), 1895 (2011).
[21] F. Lv et al., Journal of Materials Letter. **157**, 277 (2015).
[22] X. Niu et al., Journal of Optik. **126**(24), 5513 (2015).